



Original Articles

Rpn10 promotes tumor progression by regulating hypoxia-inducible factor 1 alpha through the PTEN/Akt signaling pathway in hepatocellular carcinoma



Zhiyuan Jiang^{a,1}, Qingqing Zhou^{a,1}, Chao Ge^a, Jing Yang^a, Hong Li^a, Taoyang Chen^b, Haiyang Xie^c, Ying Cui^d, Miaomiao Shao^a, Jinjun Li^a, Hua Tian^{a,*}

^a State Key Laboratory of Oncogenes and Related Genes, Shanghai Cancer Institute, Renji Hospital, Shanghai Jiaotong University School of Medicine, Shanghai, China

^b Qi Dong Liver Cancer Institute, Qi Dong, Jiangsu Province, China

^c Department of General Surgery, the First Affiliated Hospital, School of Medicine, Zhejiang University, Hangzhou, China

^d Cancer Institute of Guangxi, Nanning, China

ARTICLE INFO

Keywords:

Rpn10
HIF1 α
PTEN
Proliferation
Hepatocellular carcinoma

ABSTRACT

The ubiquitin-proteasome pathway plays a pivotal role in tumor progression. Rpn10 is the major ubiquitin (Ub) receptor of the 26S proteasome. Mounting evidence shows that Rpn10 is associated with the progression of several tumor types. However, little is known regarding the mechanistic role of Rpn10 in hepatocellular carcinoma (HCC). In this study, we found that the upregulation of Rpn10 in HCC was associated with poor prognosis. The ectopic overexpression of Rpn10 increased HCC cell proliferation, whereas silencing Rpn10 expression resulted in decreased cell proliferation. Furthermore, we demonstrated that knockdown of Rpn10 induced cell cycle arrest at G1 phase in HCC cells. In addition, we found that Rpn10 increased cell proliferation via regulation of the PTEN/Akt pathways. Knockdown of Rpn10 induced suppression of cell proliferation could be reversed by overexpressing active Akt in HCC cells. Rpn10 directly promoted PTEN degradation through the ubiquitin-proteasome system. The transcription factor HIF1 α directly bound to the Rpn10 promoter and increased its expression in HCC tissue. Moreover, we observed a significant correlation between HIF1 α expression and Rpn10 levels in HCC patients and found that the combination of these two parameters was a more powerful predictor of poor prognosis than either parameter alone. Collectively, these findings highlight the molecular mechanism of Rpn10 expression in HCC and provide valuable information for cancer prognosis and treatment.

1. Introduction

Hepatocellular carcinoma (HCC) is the most common type of primary liver cancer. HCC is the fifth most prevalent and the third most deadly type of malignant tumor worldwide. This type of tumor is particularly prevalent in Eastern Asian and Sub-Saharan African countries due to chronic hepatitis B virus (HBV) infections [1,2]. Surgical resection and liver transplantation are among the options available for the treatment of early-stage HCC [3]. Unfortunately, the prognosis of HCC remains poor because of its propensity for metastatic progression and poor response to pharmacological treatment. Therefore, the identification of potential diagnostic and therapeutic targets to improve the prognosis of HCC patients has become a critical issue.

The ubiquitin-proteasome pathway plays a pivotal role in cellular processes. It regulates the expression of many key proteins that are

involved in cell cycle progression and oncogenesis [4,5]. The 26S proteasome catalyzes the great majority (at least 80%) of protein degradation in growing mammalian cells. Two subunits of the regulatory particles, Rpn10 and Rpn13, are the major ubiquitin (Ub) receptors of the 26S proteasome [6]. Many studies have shown that Rpn10 plays an important role in tumor progression. Rpn10 is overexpressed in human colon cancer specimens [7]. Rpn10 is amplified and overexpressed in breast cancer, and its overexpression correlates with poor survival [8]. However, previous studies also showed that Rpn10 inhibited breast cancer proliferation through activation of epidermal growth factor receptor and nuclear factor kappa B (NF- κ B) [9]. Therefore, Rpn10 can play different roles in tumors depending on the type of tumor. Although it has previously been reported that expression of Rpn10 was elevated in HCC tissues [10], the function and the molecular mechanism underlying the role of Rpn10 in HCC and the relationship between its

* Corresponding author. State Key Laboratory of Oncogenes and Related Genes, Shanghai Cancer Institute, Renji Hospital, Shanghai Jiaotong University School of Medicine, 25/Ln 2200, Xietu Road, Shanghai, 200032, China.

E-mail address: htian@shsci.org (H. Tian).

¹ These authors contribute equally.

expression and clinicopathologic significance remain unclear. In this study, we explored the regulatory mechanism of Rpn10 expression in HCC. The role of Rpn10 in HCC progression was also investigated, along with its underlying molecular mechanisms.

2. Materials and methods

2.1. Cell lines and cell culture

Huh7 cells were obtained from Riken Cell Bank (Tsukuba, Japan). PLC/PRF/5, SK-Hep1 and HEK-293T cell lines were purchased from the American Type Culture Collection (Manassas, VA, USA). The HCC-LM3 cell line was obtained from the Liver Cancer Institute, Zhongshan Hospital of Fudan University (Shanghai, China). The HCC-LY10 cell line was established in our laboratory. SMMC-7721 and L02 were obtained from the Cell Bank of the Institute of Biochemistry and Cell Biology, China Academy of Sciences (Shanghai, China). The HCC cell lines used in this study were cultured in Dulbecco's modified Eagle's medium (DMEM) (HyClone) containing 10% heat-inactivated fetal bovine serum (Gibco) and incubated at 37 °C in a humidified atmosphere with 5% CO₂. The chemicals and other reagents were purchased from Sigma-Aldrich unless otherwise specified.

2.2. Vector constructs, lentivirus production, and cell transduction

The Rpn10 plasmid and HIF1 α lentiviral shRNA plasmid were supplied by Genechem (Shanghai, China). The Rpn10 lentiviral shRNA plasmid was supplied by GeneCopoeia (Guangzhou, China). The target sequences are listed in [Supplementary Table 1](#). A constitutively active form of Akt (Myr-Akt) was constructed in our laboratory [11]. Viral packaging was performed in HEK-293T cells after cotransfection of the pWPXL-Rpn10 vector with the packaging plasmid psPAX2 and the envelope plasmid pMD2.G (Addgene) using Lipofectamine 2000 (Invitrogen). The viruses were harvested 72 h after transfection, and the viral titers were determined. HCC cells were infected with 1×10^6 recombinant lentivirus-transducing units in the presence of 6 μ g/ml polybrene (Sigma).

2.3. Quantitative real-time RT-PCR (qRT-PCR)

Total RNA extraction, reverse transcription, and qRT-PCR analyses were performed as previously described using an ABI Prism 7500 System (Applied Biosystems, Carlsbad, CA, USA) with SYBR[®] Premix Ex Taq (Takara, Dalian, China) [12]. The primer sequences are listed in [Supplementary Table 2](#).

2.4. Western blotting

Cell lysates were separated by SDS-polyacrylamide gel electrophoresis and transferred onto nitrocellulose membranes. The membranes were incubated overnight with primary antibodies at 4 °C. The membranes were then probed with HRP-conjugated secondary antibodies. The immunoreactive blots were visualized using an enhanced chemiluminescence reagent (Pierce, Rockford, IL, USA). β -actin was used as a loading control. Information on the antibodies is listed in [Supplementary Table 3](#).

2.5. Cell proliferation and colony formation assays

Cell proliferation was measured by the Cell Counting Kit-8 (CCK8) (Bimake, USA) according to the manufacturer's instructions. For colony formation assays, 1000 cells were plated in each well of a 6-well plate and incubated at 37 °C for 2 weeks. Colonies were fixed with 4% phosphate-buffered formalin (pH 7.4) and Giemsa stained for 15 min. Each experiment was performed in triplicate.

2.6. Cell cycle analysis

For cell cycle analysis, cells were placed in a 6-well culture plate and grown for 24 h. The cells were trypsinized, washed twice with cold PBS and fixed with cold 70% ethanol at –20 °C overnight. The cells were then washed twice with PBS and incubated with 10 mg/ml RNase A, 400 mg/ml propidium iodide and 0.1% Triton X in PBS at 4 °C for 30 min. Finally, the cells were analyzed by flow cytometry. Cell cycle profile distributions were determined with Modfit LT 3.2 software.

2.7. Immunofluorescent confocal imaging

Briefly, cells were seeded onto glass slides for 24 h, and then subjected to hypoxia (1% O₂) for 24 h. Afterward, the cells were fixed in 4% paraformaldehyde and permeabilized with 0.5% Triton X-100 for 15 min. The slides were then incubated with primary antibodies in blocking solution overnight at 4 °C in a humidified chamber. Subsequently, the glass slides were washed three times in PBS and incubated in Alexa Fluor 594-conjugated and Alexa Fluor 488-conjugated secondary antibody and 4',6-diamidino-2-phenylindole (DAPI) in blocking solution for 30 min at 37 °C in a humidified chamber. Images were obtained with a Leica TCS SP8 confocal system (Leica, Microsystems).

2.8. Immunohistochemistry (IHC)

A tissue microarray containing 118 HCC tissues was used for immunohistochemical procedures. IHC assays were conducted as reported previously [13]. Briefly, the sections were deparaffinized with xylene and rehydrated before being heated to just below boiling temperature at a subboiling temperature in sodium citrate buffer (pH 6.0) for 20 min in a microwave oven for antigen retrieval. After being washed with PBS three times, the samples were incubated with 3% hydrogen peroxide for 10 min to block endogenous peroxidase activity. The sections were then incubated overnight at 4 °C with antibodies against Rpn10 and HIF1 α . After being rinsed with PBS, the sections were incubated with horseradish peroxidase (HRP)-conjugated secondary antibody was applied at 37 °C for 30 min and then incubated with diaminobenzidine solution. Finally, the nuclei were counterstained with Mayer's hematoxylin.

2.9. Chromatin immunoprecipitation (ChIP) assay

ChIP assays were performed with a ChIP assay kit (Upstate Biotechnology) following the manufacturer's instructions as described previously [13]. HCC cells treated with or without hypoxia were grown to 90% confluence, and crosslinking was performed with 1% formaldehyde for 10 min. The cell lysates were sonicated to shear the DNA to sizes of 500 to 1000 bp. Mouse anti-HIF1 α or mouse IgG was used to immunoprecipitate DNA-containing complexes. After reverse cross linking of protein/DNA complexes to free DNA, qRT-PCR was used to detect the HIF1 α -binding site in Rpn10 promoter region. The primer sequences are listed in [Supplementary Table 2](#).

2.10. GST pull-down assay

GST-PTEN fusion protein and GST fusion protein were purchased from Proteintech Group (Proteintech, Ag17274 and Ag25094). GST pull-down assay was performed according to the earlier described method [14]. In brief, the beads with GST or GST-PTEN fusion protein were incubated with Huh7 whole-cell proteins for 2 h at 4 °C. The supernatant was removed. The beads were then washed with the reaction buffer 4 times. The target proteins were collected and detected using Western blotting assays.

2.11. Co-Immunoprecipitation (Co-IP) assay

Co-IP assays were performed using Huh7 and HCC-LM3 cells. The cells were harvested in RIPA (Upstate, Biotechnology) lysis buffer for 40 min on ice and centrifuged at 12 000 g for 10 min. The protein A/G agarose beads were incubated with antibody against PTEN and Rpn10 or negative control IgG overnight at 4 °C while rotating. After washing, the complexes were subjected to western blotting analysis.

2.12. Statistical analysis

Statistical analyses were performed using SPSS16.0 software. All data are presented as the mean \pm SD. Pairwise comparisons were conducted using the two-tailed Student's t-test. Comparisons among three or more group comparisons were conducted using one-way ANOVA. Chi Square tests were used to analyze the relationships between the expression of Rpn10 and the clinicopathologic features. The Kaplan-Meier method was used to plot survival curves, which were compared by the log-rank test. The prognostic significance of Rpn10 was evaluated by univariate and multivariate Cox regression analyses. $p < 0.05$ was considered statistically significant.

3. Results

3.1. High expression of Rpn10 predicts a poor prognosis in HCC

We first detected the expression of Rpn10 in human HCC tissues. Our results showed that expression of Rpn10 was upregulated in HCC tissues compared with noncancerous tissues (Fig. 1A). To confirm this result, we analyzed the expression levels of Rpn10 using data sets from TCGA (The Cancer Genome Atlas) and GEO (Gene Expression Omnibus). The results showed that the expression of Rpn10 was upregulated in HCC based on the TCGA and GEO databases (Fig. 1B and C). Moreover, Rpn10 protein levels were upregulated in HCC tissues compared with noncancerous tissues according to Western blot results (Fig. 1D).

Apart from HCC, data retrieved from TCGA also revealed that Rpn10 overexpression is present in other solid cancers, including bladder urothelial carcinoma (BLCA), breast invasive carcinoma (BRCA), colon adenocarcinoma (COAD), esophageal cancer (ESCA), kidney renal clear cell carcinoma (KIRC), kidney renal papillary cell carcinoma (KIRP), lung adenocarcinoma, mesothelioma (MESO), stomach adenocarcinoma (STAD), and prostate adenocarcinoma (PRAD) (Supplementary Fig. 1A).

Because the expression of Rpn10 was upregulated in tumors derived from several different tissue types, we next investigated the clinical significance of Rpn10 in HCC patients (Supplementary Table 4). The results showed that Rpn10 expression was positively associated with gender and HBV positive. However, there was no correlation between Rpn10 expression and other clinicopathological factors, including age, Edmondson's grade, Cirrhosis, serum alpha-fetoprotein (AFP) and intrahepatic metastasis (Supplementary Table 5). The Kaplan-Meier survival analysis revealed that higher levels of Rpn10 were associated with a shorter overall survival (OS) time ($p = 0.039$; Fig. 1E and F). Furthermore, multivariate COX proportional hazard analysis suggested that high expression Rpn10 was associated with worse survival of HCC patients (HR = 2.260, 95% CI = 1.025 – 4.980, $p = 0.043$; Supplementary Table 6). The results from the TCGA HCC cohort demonstrated that HCC patients in the group with high Rpn10 expression group had shorter overall survival than the low-expression group (log-rank, $p = 0.009$) using Kaplan-Meier analysis (Fig. 1G). In addition, kidney renal clear cell carcinoma (KIRC), mesothelioma (MESO), kidney renal papillary cell carcinoma (KIRP) and uveal melanoma (UVM) patients in the high-Rpn10-expression group had shorter overall survival than the low-expression group (log-rank, $p < 0.05$) using Kaplan-Meier analysis (Supplementary Fig. 1B). Thus, these findings

suggest that Rpn10 could serve as a valuable predictive factor for cancer patients, including HCC.

3.2. Rpn10 promotes HCC cell proliferation

To verify the role of Rpn10 in HCC progression, we first examined the expression of Rpn10 in HCC cell lines. We selected SMMC-7721, Huh7, PLC/PRF/5, and HCC-LM3 cell lines for the establishment of an in vitro proliferation model with various Rpn10 expression levels (Fig. 2A). Our results showed that the exogenous expression of Rpn10 promoted cell growth and colony formation compared to the levels in vector control cells (Fig. 2B–D, Supplementary Fig. 2A). Conversely, Rpn10 knockdown inhibited HCC cell proliferation and colony formation (Fig. 2E–G, Supplementary Fig. 2B). Overall, our results suggest that Rpn10 plays a critical role in the proliferation of HCC cells.

3.3. Rpn10 regulates the G1-S phase transition and alters the expression of cell-cycle regulators in HCC cells

To further investigate the mechanism by which Rpn10 affects HCC proliferation, we determined the cell cycle distributions of Huh7 and HCC-LM3 cells by flow cytometry. Our results showed that knockdown of Rpn10 increased the proportion of cells entering the G1 phase and decreased the proportion of cells entering the S phase, indicating that knockdown of Rpn10 induces cell cycle arrest at G1 phase in Huh7 and HCC-LM3 cells (Fig. 3A). The expression levels of CDK4, CDK6, cyclinD1, phosphorylated Rb (Ser807/811) and proliferating cell nuclear antigen (PCNA) were increased in Rpn10-overexpressing cells compared to control cells (Fig. 3B). Conversely, the expression levels of CDK4, CDK6, cyclinD1, phosphorylated Rb (Ser807/811) and PCNA were reduced in Rpn10-knockdown cells compared to control cells (Fig. 3C). However, the expression of E2F1 did not change in Rpn10-overexpressing and Rpn10-knockdown HCC cells. Therefore, all results suggest that Rpn10 promotes the proliferation of cells by inducing cell cycle G1/S transition in HCC cells.

3.4. Rpn10 promotes HCC cell proliferation through the PTEN/Akt pathways

Given that the PI3K/Akt pathway plays an important role in HCC cell proliferation, we next sought to determine whether this pathway might have a role in Rpn10-induced cell proliferation [15]. Our results showed that overexpression of Rpn10 increased the phosphorylation of Akt in HCC cells (Fig. 4A, Supplementary Fig. 3A). In contrast, Akt phosphorylation was inhibited in Rpn10-knockdown HCC cells (Fig. 4B, Supplementary Fig. 3B). To confirm the role of Akt in Rpn10-mediated HCC proliferation, we tested the effect of expressing constitutively active Akt (Myr-Akt) on the cell proliferation capacity of Rpn10 knockdown cells. The results showed that knockdown of Rpn10 induced suppression of cell proliferation could be reversed by overexpressing active Akt in HCC cells (Fig. 4C–E, Supplementary Fig. 3C). Therefore, these results suggested that Rpn10 promoted cell proliferation through the PI3K/Akt pathway in HCC cells.

3.5. Rpn10 inhibits PTEN expression via the ubiquitin-proteasome pathway in HCC cells

PTEN negatively regulates the PI3K/Akt pathway [16]. Therefore, we detected PTEN expression in Rpn10-overexpressing and Rpn10-knockdown HCC cells. Our results showed that overexpression of Rpn10 decreased the expression of PTEN in HCC cells (Fig. 4A, Supplementary Fig. 3A). Conversely, knockdown of Rpn10 increased the expression of PTEN protein in HCC cells (Fig. 4B, Supplementary Fig. 3B). However, Rpn10 did not affect the expression of PTEN mRNA in HCC cells (Fig. 4F).

To confirm the influence of Rpn10 on PTEN stability, we incubated

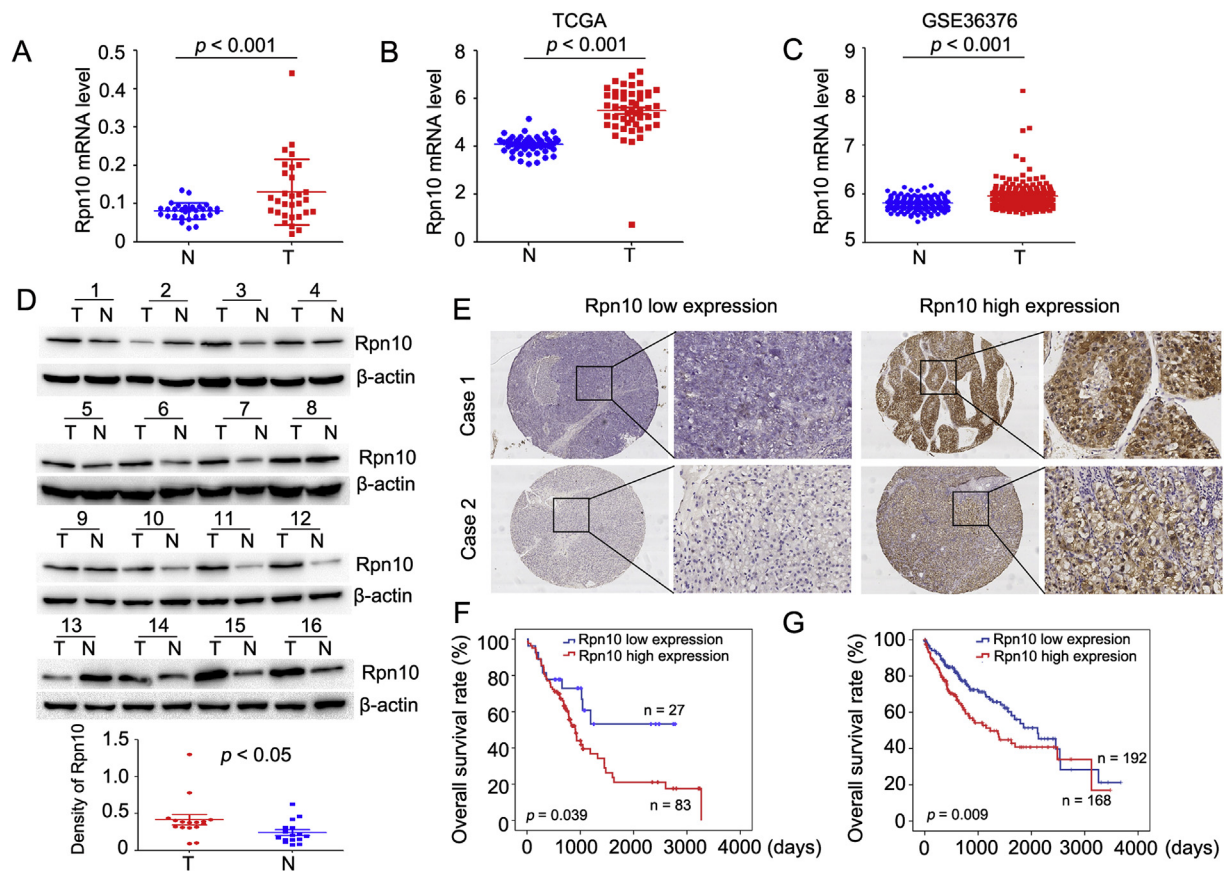


Fig. 1. Rpn10 is often upregulated in HCC and is associated with poor prognosis in HCC patients. (A) qRT-PCR analysis of Rpn10 expression in HCC tissues compared with paired corresponding noncancerous liver tissues ($n = 30$) (T, tumor; N, noncancerous liver tissue). (B) The expression of Rpn10 in HCC tissues compared with paired corresponding noncancerous liver tissues was analyzed using data sets from TCGA ($n = 50$). (C) The expression of Rpn10 in HCC tissues compared with noncancerous liver tissues was analyzed using data sets from GEO. (D) Western blot analysis of Rpn10 expression in HCC tissues compared with paired corresponding noncancerous liver tissues. (E) IHC analysis of Rpn10 expression in 118 HCC samples. Representative images are shown. (F) Overall survival analysis of HCC patients with Rpn10 expression. (G) Patients with high expression levels of Rpn10 had shorter overall survival than patients with low expression levels as determined using data sets from TCGA.

Rpn10-knockdown or control HCC cells in cycloheximide (50 $\mu\text{g}/\text{ml}$), which blocks de novo protein synthesis. The results showed that in the presence of cycloheximide, knockdown of Rpn10 resulted in a slow rate of PTEN degradation compared with the rate in control cells, suggesting that expression of Rpn10 protein decreases the stability of PTEN protein (Fig. 4G). The half-life of the PTEN protein in the cells was extended from 3 to 12 h as a consequence of Rpn10 knockdown (Fig. 4G).

To investigate the involvement of the ubiquitin-proteasome pathway in the proteolytic degradation of PTEN, we applied MG132, a reversible inhibitor of proteasome, to Rpn10-overexpressing HCC cells. Our results showed that PTEN degradation induced by Rpn10 overexpression was inhibited in the presence of the proteasome inhibitor MG132 (Fig. 4H, Supplementary Fig. 3D). In addition, overexpression of Rpn10 resulted in the accumulation of ubiquitinated PTEN (Fig. 5A). We conclude that the Rpn10 inhibits PTEN expression via the ubiquitin-proteasome pathway in HCC cells.

To elucidate the molecular mechanism of Rpn10-mediated PTEN degradation, we examined whether Rpn10 could interact with PTEN. Our results show that Rpn10 interacts with PTEN directly in the Co-IP and GST pull-down assay (Fig. 5B–D).

In addition, we conducted immunofluorescence staining to assess a potential colocalization between Rpn10 and PTEN. Our results demonstrated that Rpn10 and PTEN were co-localized in Huh7 and HCC-LM3 cells (Fig. 5E). Moreover, Rpn10 and PTEN interaction was increased slightly in MG132-treated cells (Fig. 5E). Subsequently, we analyzed the relationship between Rpn10 and PTEN in human primary

HCC tissues. Our results showed that there was a significantly negative correlation between the expression of Rpn10 and PTEN protein level in HCC tissue (Fig. 5F).

3.6. Rpn10 expression is induced by hypoxia in HCC cells

Hypoxia plays an important role in the development and progression of HCC, and we next sought to determine whether Rpn10 expression could be induced by hypoxia in HCC cells. To confirm the effects of hypoxia on Rpn10 expression, we subjected SMMC-7721 and PLC/PRF/5 cells to hypoxia (1% O_2) to mimic a hypoxic microenvironment. Our results showed that Rpn10 expression was upregulated in hypoxia-treated HCC cells (Fig. 6A and B, Supplementary Fig. 4A). Furthermore, the immunofluorescence results also showed that hypoxia induced Rpn10 expression in HCC cells. Furthermore, there was a colocalization between Rpn10 and HIF1 α in SMMC-7721 and PLC/PRF/5 cells (Fig. 6C). To evaluate the expression of Rpn10 depending on the hypoxia-induced microenvironment, we detected the expression of Rpn10 in SMMC-7721 orthotopic liver tumors [17]. Our results showed that the expression of Rpn10 colocalized with that of HIF1 α in SMMC-7721 orthotopic liver tumor tissues. Furthermore, Rpn10 expression was higher in tumor tissue with higher HIF1 α expression (Fig. 6D). Furthermore, the same results were shown in the Human Protein Atlas (Supplementary Fig. 5, www.proteinatlas.org). To further clarify the role of HIF1 α in regulating Rpn10 expression, we knocked down HIF1 α using shRNA in SMMC-7721 and PLC/PRF/5 cells. Our results showed

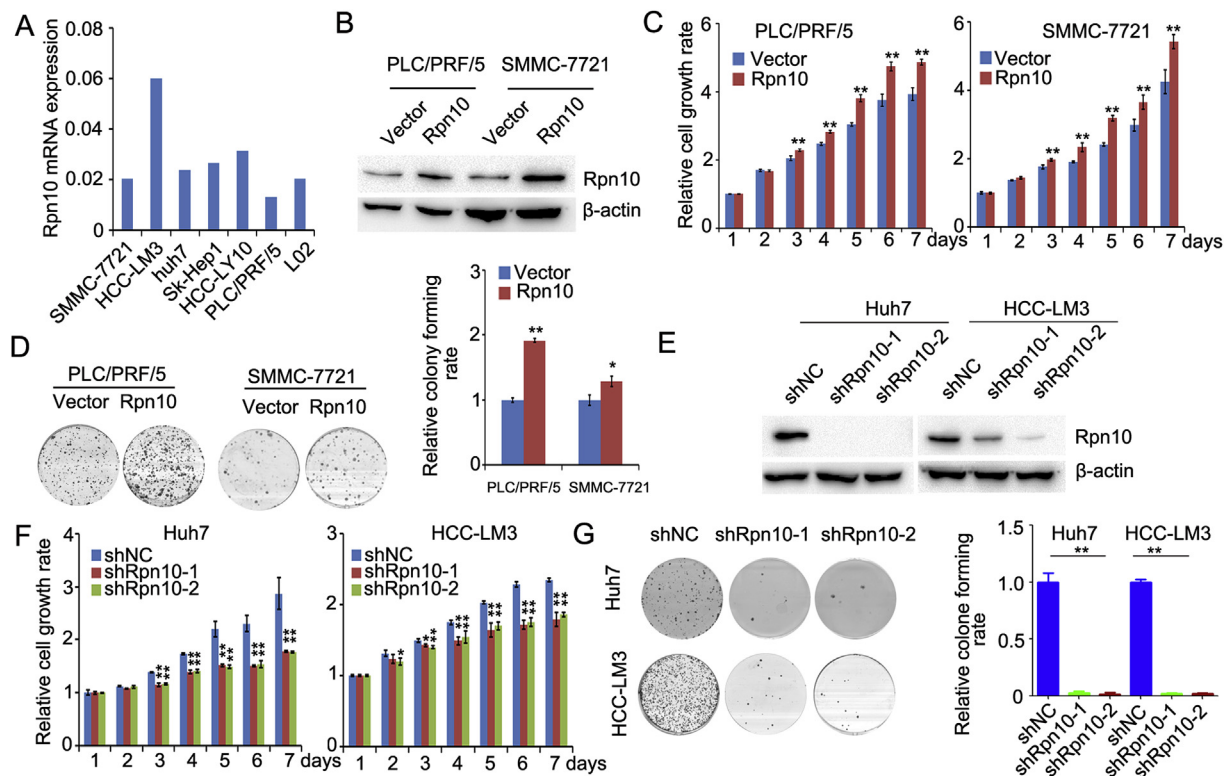


Fig. 2. Rpn10 increases HCC cell proliferation. (A) Expression of Rpn10 mRNA in HCC cell lines was detected by qRT-PCR. (B) The expression level of Rpn10 was detected by Western blotting in Rpn10-overexpressing HCC cells. (C) The effect of Rpn10-overexpressing on HCC cell proliferation was assessed by a CCK8 assay. (D) The effect of Rpn10-overexpressing on HCC cell proliferation was assessed by a colony formation assay. (E) The expression level of Rpn10 was detected by Western blotting in Rpn10 knockdown HCC cells. (F) The effect of Rpn10 knockdown on HCC cell proliferation was assessed by a CCK8 assay. (G) The effect of Rpn10 knockdown on HCC cell proliferation was assessed by a colony formation assay. * $p < 0.05$; ** $p < 0.01$.

that hypoxia-induced upregulation of Rpn10 could be partially reversed by the knockdown of HIF1 α (Fig. 6E, Supplementary Fig. 4B). Therefore, these results indicate that hypoxia-induced Rpn10 expression is dependent on HIF1 α in HCC cells.

3.7. HIF1 α binds to the Rpn10 promoter and increases the expression of gene in HCC cells

Based on the above mentioned results, we speculated that HIF1 α can bind to the Rpn10 promoter and increase the expression of the gene. Five potential hypoxia-responsive elements (HREs) within a 1.5 kb (kilobase) region upstream of the transcriptional start site of Rpn10 were identified by bioinformatics analysis (Fig. 6F and G). ChIP assay analysis showed that the anti-HIF1 α antibody could precipitate HRE1/2 (–121 to –131, –144 to –155), but not other HREs (Fig. 6H, Supplementary Fig. 6). Furthermore, bioinformatics analysis showed that HRE1 and HRE2 are conserved, but not other HREs in human and mouse Rpn10 promoter (Supplementary Fig. 7). All these results indicate that HIF1 α binds to the Rpn10 promoter and increases the expression of the gene in HCC.

To further explore potential clinical applications of the experimental data, we next assessed the expression of HIF1 α in HCC based on the TCGA and GEO. The results showed that expression of HIF1 α was upregulated in HCC tissues compared with noncancerous tissues (Fig. 7A and B). Subsequently, we analyzed the relationship between Rpn10 and HIF1 α mRNA in human primary HCC tissues using data sets from TCGA and GEO. Our results showed that there was a significant positive correlation between the expression of HIF1 α and Rpn10 in HCC tissue (Fig. 7C and D). Next, we analyzed the relationship between Rpn10 and HIF1 α protein level in human primary HCC tissues. Our results showed that there a significant positive correlation between the

expression of HIF1 α and Rpn10 in HCC tissue ($r = 0.496$, $p < 0.01$; Fig. 7E and F).

3.8. High expression of Rpn10 and HIF1 α in HCC predicts a poor prognosis

We next investigated the clinical significance of HIF1 α in HCC based on TCGA. The results showed that HCC patients with high HIF1 α expression had shorter overall survival than the low-expression group (log-rank, $p = 0.003$) using Kaplan-Meier analysis (Fig. 7G).

Accumulating evidence indicates that a combination of multiple markers might be more informative than any single marker for predicting patient prognoses. Based on the expression of Rpn10 and HIF1 α , HCC patients were classified into the following two groups: a group with low Rpn10 and low HIF1 α group ($n = 20$) and one with high Rpn10 and high HIF1 α ($n = 64$). The patients with high expression of Rpn10 and HIF1 α displayed a worse prognosis than the low Rpn10 and HIF1 α groups (Fig. 7H). In addition, the patients with high expression of Rpn10 and HIF1 α displayed a worse prognosis than the low Rpn10 and HIF1 α groups based on TCGA, indicating that the combination of Rpn10 and HIF1 α has better prognostic value than Rpn10 or HIF1 α alone (Fig. 7I).

4. Discussion

In the present work, we show that hypoxia-induced Rpn10 expression is mediated by a HIF1 α -dependent mechanism. Furthermore, the transcription factor HIF1 α directly binds to the Rpn10 promoter and promotes the expression of the gene in HCC. High expression of both Rpn10 and HIF1 α predicts worse prognosis than high expression of either Rpn10 or HIF1 α alone in HCC patients. In addition, Rpn10 promotes the G1/S cell cycle transition by activating Akt to promote

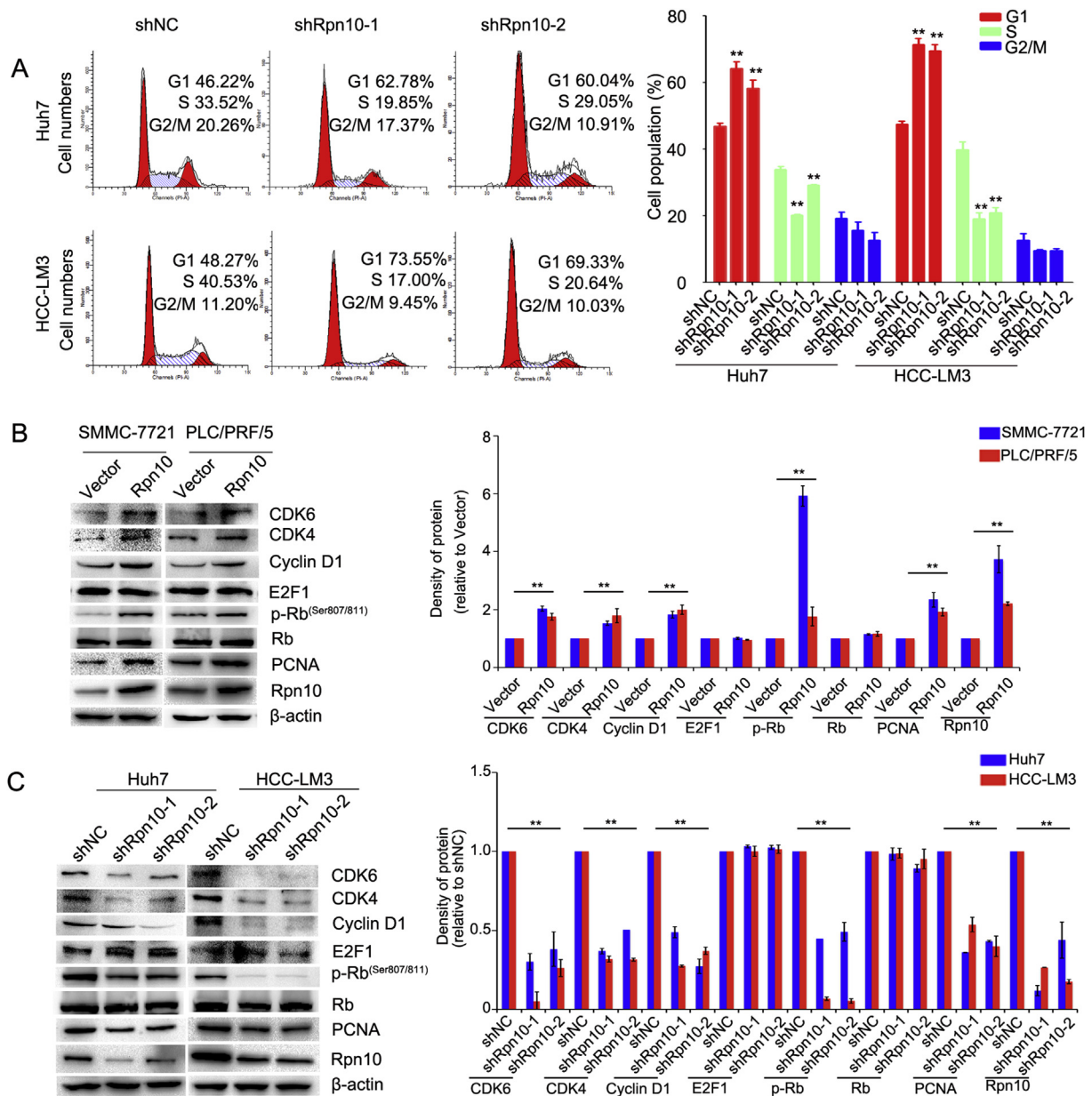


Fig. 3. Effect of Rpn10 on the cell cycle and cell cycle-related protein expression. (A) The cell cycle distribution of Rpn10 knockdown Huh7 and HCC-LM3 cells was analyzed by flow cytometry. $**p < 0.01$. (B) Expression of CDK4/6, cyclin D1, PCNA, p-Rb, Rb, E2F1 and Rpn10 was detected by Western blotting in Rpn10-overexpressing SMMC-7721 and PLC/PRF/5 cells. (C) The expression of CDK4/6, cyclin D1, PCNA, p-Rb, Rb, E2F1 and Rpn10 was detected by Western blotting in Rpn10 knockdown Huh7 and HCC-LM3 cells.

cell growth in HCC.

A previous study showed that Rpn10 expression was elevated in tumor tissues, but the mechanism and factors affecting Rpn10 expression in tumors are not clear. Lin et al. reported that transcription factor nuclear factor erythroid 2-related factor 2 (Nrf2) promotes colorectal cancer with more aggressive tumors via upregulation of Rpn10 [18]. Hypoxia is a common feature of human solid tumors [19]. Hypoxia is considered to be involved in HCC development. A large body of evidence shows that hypoxia plays an important role in the regulation of proliferation and metastasis that it predicts a poor prognosis [20,21]. Moreover, previous studies have shown that HIF1α plays an important role in the development of HCC by promoting HCC metastasis, EMT and prognosis [22,23]. In addition, genetic variations of HIF-1α have been associated with an increased risk of development and prognosis of HCC and could serve as biomarkers [24]. The transcription factor HIF1α regulates several cellular signaling events by binding to specific DNA

sequences known as hypoxia responsive elements (HREs) in target genes, directly increasing or decreasing their expression [25]. These results strongly suggest a pathological role of HIF1α in HCC development and progression. In the present study, Rpn10 expression was increased in hypoxia-treated HCC cells. We also verified HIF1α as a key upstream regulatory factor of Rpn10 in that HIF1α can directly bind to the promoter of that gene, leading to increased expression of Rpn10 in HCC cells. Moreover, there was a positive correlation between the expression levels of Rpn10 and HIF1α in HCC cells both *in vitro* and *in vivo*. Therefore, these data indicated that downregulation of Rpn10 in hypoxic tumor areas is a valid strategy to reduce HIF1α signaling in HCC.

To date, the regulatory mechanism of Rpn10 remains largely unclear in HCC. Previous studies have shown that Rpn10 can bind to death receptor-6 (DR6) and thereby induce human acute monocytic leukemia cells to differentiate [26]. Knockdown of Rpn10 inhibits p53 protein

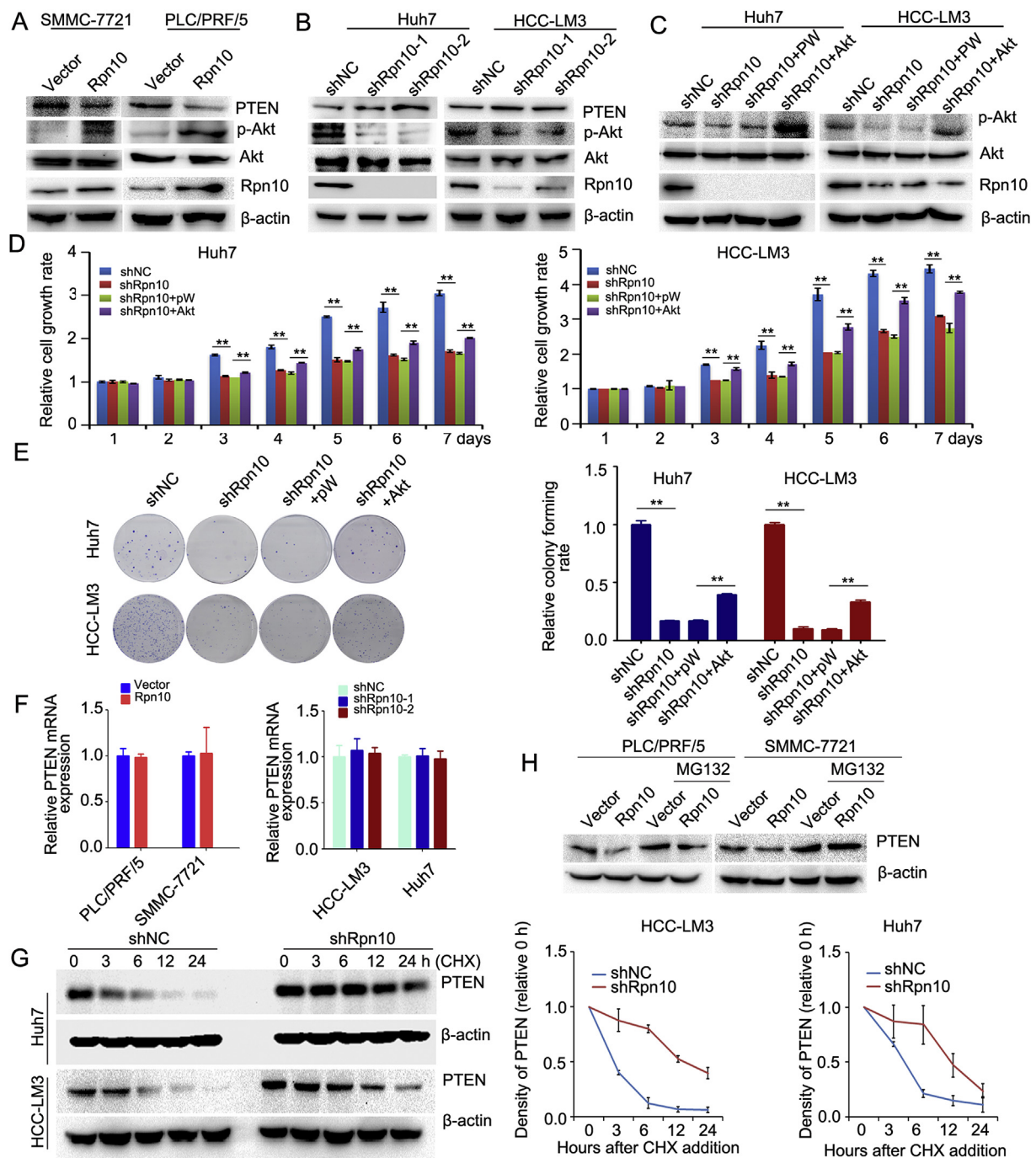


Fig. 4. Rpn10 increased cell proliferation through the PTEN/Akt pathway. (A) Expression of p-Akt, Akt, PTEN and Rpn10 in Rpn10-overexpressing SMMC-7721 and PLC/PRF/5 cells. (B) Expression of p-Akt, Akt, PTEN and Rpn10 in Rpn10 knockdown Huh7 and HCC-LM3 cells. (C) Rpn10-knockdown HCC-LM3 and Huh7 cells were transfected with active Akt as indicated, and p-Akt expression was detected by Western blotting. (D) Rpn10 knockdown cells (Huh7 and HCC-LM3) were transfected with active Akt as indicated, and proliferation of cells was assessed by a CCK8 assay. (E) Rpn10 knockdown cells (Huh7 and HCC-LM3) were transfected with active Akt as indicated, and proliferation of cells was assessed by a colony formation. (F) Expression of PTEN mRNA in Rpn10-overexpressing and Rpn10-knockdown HCC cells. (G) Expression of PTEN in Rpn10-knockdown HCC cells treated with cycloheximide (CHX) at the indicated time points. (H) Expression of PTEN in Rpn10-overexpressing HCC cells treated with MG132 for 6 h**p < 0.01.

degradation and results in the accumulation of ubiquitinated p53 [27]. In this study, we found that the expression of p53 protein did not change in either gain-of-function or loss-of-function analyses of Rpn10 in human HCC cell lines (data not shown). However, we found that the proliferative activity of Rpn10 is mediated by the PTEN/Akt pathway. Increasing evidence suggests that the PTEN/Akt pathway plays a central role in a variety of oncogenic processes, including cell growth, proliferation, metastasis, angiogenesis, and metabolism [11,28]. Rpn10

serves as a 26S proteasome which catalyzes much the protein degradation in growing mammalian cells [27,29].

It has been reported previously that Rpn10 could regulate the proliferation of cancer cells. In this study, we find that knockdown of Rpn10 inhibits HCC cells proliferation by inhibiting the expression of cyclin D1 and CDK4/6. Cyclin D1 and CDK4/6 are key protein in G1/S checkpoint. Phosphorylation of the Rb protein by cyclin D-CDK4/6 inactivates the growth-inhibitory function of Rb during the G1 phase

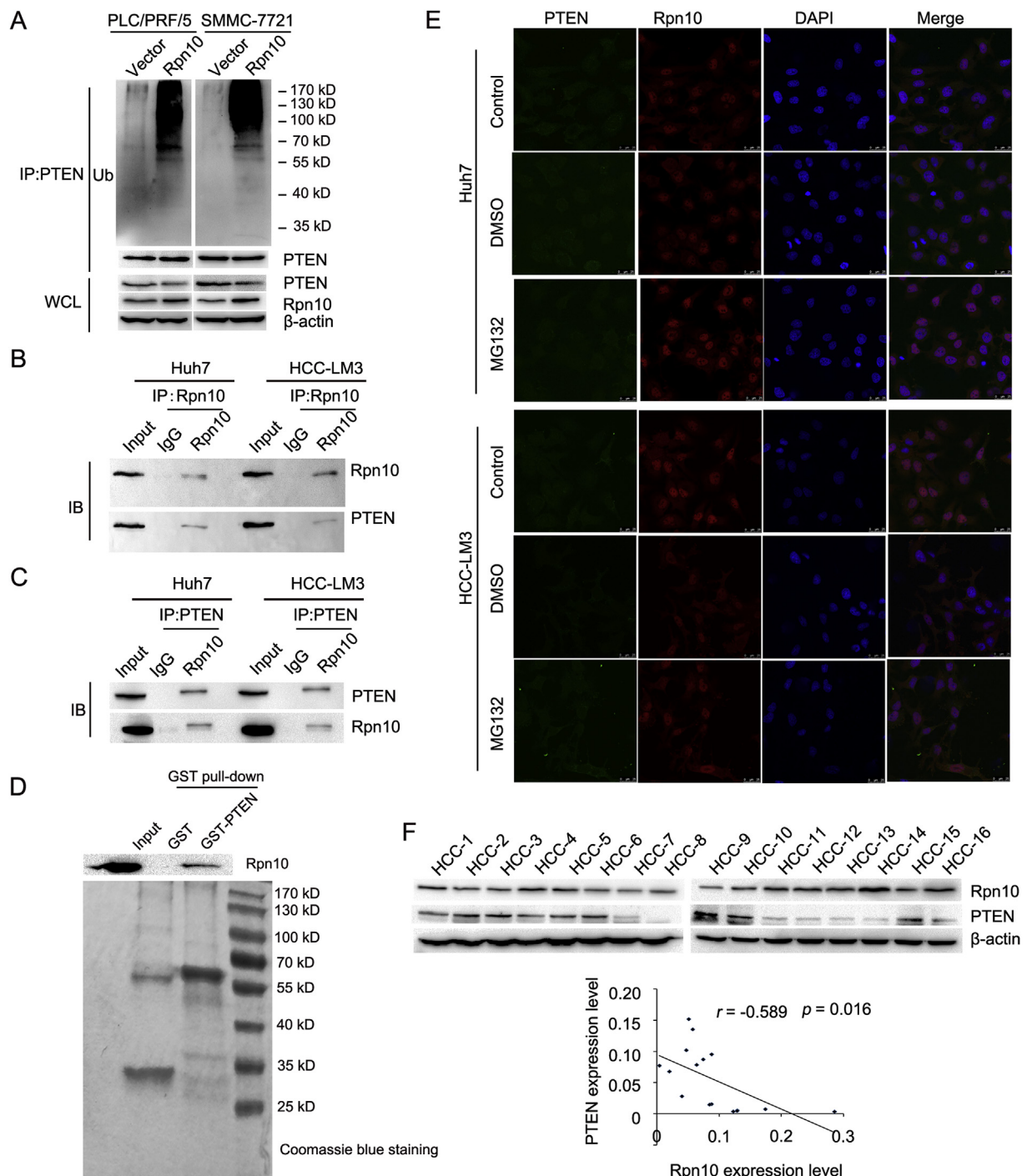


Fig. 5. Rpn10 binds PTEN and associates with ubiquitination. (A) Cell lysates of Rpn10-overexpressing and control PLC/PRF/5 and SMMC-7721 cells were immunoprecipitated with anti-PTEN antibody, and the immunocomplexes were immunoblotted with antibodies against ubiquitination. (B) Endogenous PTEN was immunoprecipitated with anti-Rpn10 antibody, with IgG as the negative control, and immunocomplexes were analyzed with WB with anti-Rpn10 and anti-PTEN antibodies. (C) Endogenous Rpn10 was immunoprecipitated with anti-PTEN antibody, with IgG as the negative control, and immunocomplexes were analyzed with WB with anti-Rpn10 and anti-PTEN antibodies. (D) GST and GST-PTEN fusion proteins were immobilized on glutathione-sepharose beads and incubated with Huh7 and HCC-LM3 cell lysates at 4 °C overnight. Rpn10 was detected with WB. Purified GST and GST-PTEN were detected with Coomassie blue staining. (E) Expression of Rpn10 and PTEN protein was determined by immunofluorescent assays in Huh7 cells treated with or without MG132. (F) Western blot analysis of Rpn10 and PTEN expression in HCC tissues. The correlation between Rpn10 expression and PTEN protein level in 16 HCC tissues was analyzed. (For interpretation of the references to color in this figure legend, the reader is referred to the Web version of this article.)

[30]. The PI3K/Akt pathway is a strong activator of cyclin D1, a critical player in cell cycle progression [31]. In the present study, phosphorylation of the Akt was decreased in Rpn10 knockdown cells. These results indicate that Rpn10 regulates HCC cells proliferation through Akt-mediated cell cycle progression.

In this study, we found that the decrease in PTEN in Rpn10-overexpressing cells was not due to a transcriptional effect. Our results showed that PTEN decayed rapidly in control cells treated with the protein synthesis inhibitor CHX compared with Rpn10 knockdown cells. Furthermore, degradation of PTEN induced by Rpn10

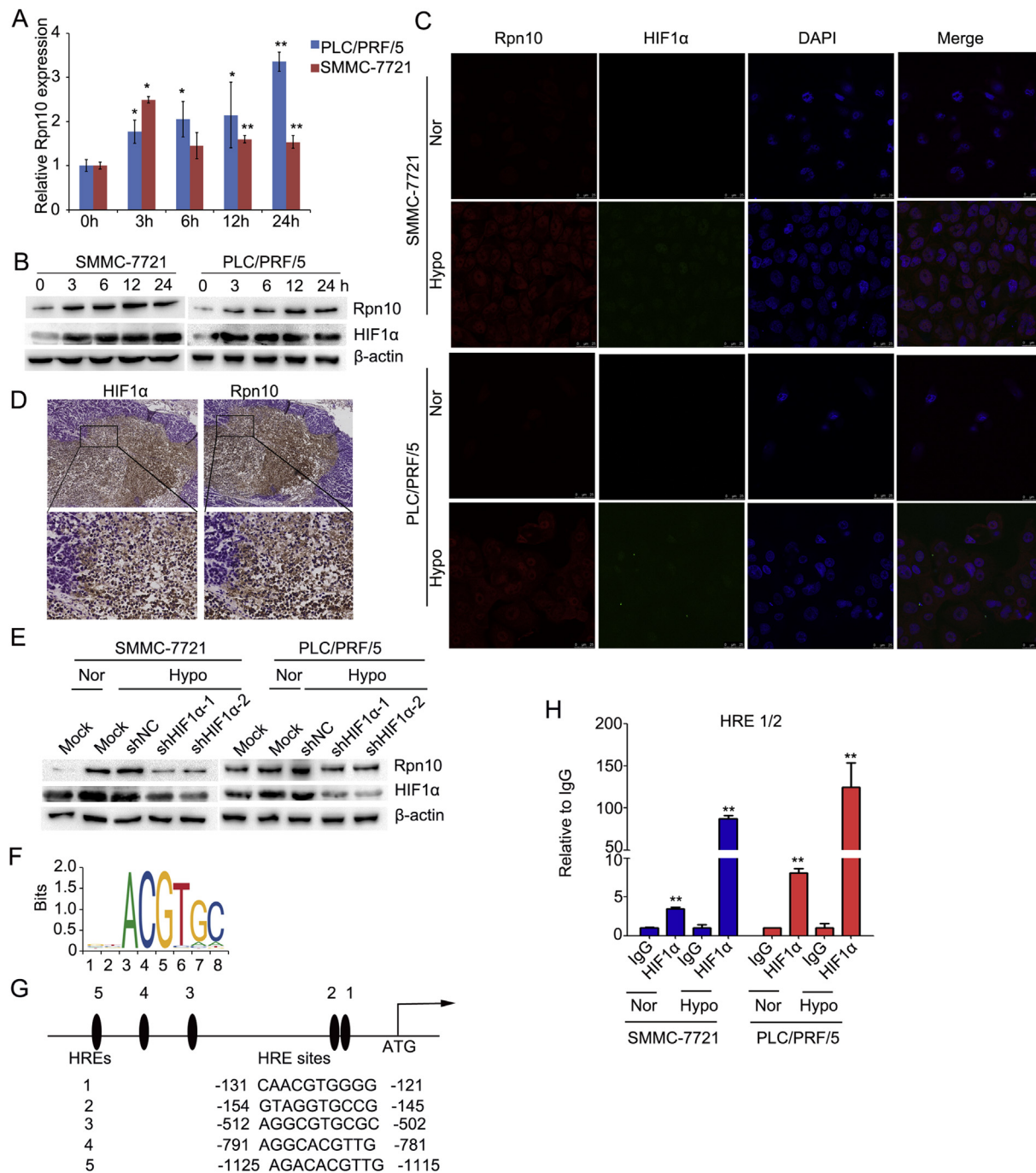


Fig. 6. HIF1 α binds to the Rpn10 promoter and increases Rpn10 expression. (A) Relative mRNA expression of Rpn10 was determined by qRT-PCR in SMMC-7721 and PLC/PRF/5 cells cultured under hypoxic conditions for the indicated amounts of time. (B) Expression of Rpn10 protein was determined by Western blotting in SMMC-7721 and PLC/PRF/5 cells cultured under hypoxic conditions for the indicated amounts of time. (C) Expression of Rpn10 and HIF1 α protein was determined by immunofluorescent assays in SMMC-7721 and PLC/PRF/5 cells cultured under hypoxic conditions for 24 h. (D) Immunohistochemical analysis of Rpn10 and HIF1 α in orthotopic liver tumors formed by SMMC-7721 cells. (E) Expression of Rpn10 and HIF1 α in HIF1 α -knockdown of SMMC-7721 and PLC/PRF/5 cells under hypoxia (Hypo) or normal oxygenation (Nor). (F) HIF1 α binding motif. (G) JASPAR analysis showed five potential HREs within the 1.5-kb region upstream of the transcriptional start site of Rpn10. (H) ChIP analysis of HIF1 α binding to the Rpn10 promoter (HRE1/2). SMMC-7721 and PLC cells were crosslinked to DNA, and chromatin-protein complexes were immunoprecipitated with an antibody against HIF1 α . * p < 0.05; ** p < 0.01.

overexpression was inhibited in the presence of the proteasome inhibitors MG132. In addition, we found that overexpression of Rpn10 increased the ubiquitinated PTEN level in HCC cells. Therefore, we speculate that Rpn10-mediated proteasome degradation of PTEN could require PTEN ubiquitination. Previous studies showed that E3 ligases (NEDD4, XIAP, CHIP, etc.) had been proposed to ubiquitinate PTEN [14,32,33]. Therefore, it will be interesting to explore this issue in

future studies. Therefore, all results suggest that Rpn10 directly degrades PTEN through the ubiquitin-proteasome pathway.

In conclusion, our observations demonstrate that overexpression of Rpn10 increases HCC cells proliferation by leading to G1/S cell phase transition. Furthermore, Rpn10 positively regulates Akt phosphorylation by degrading PTEN protein stability. The transcription factor HIF1 α binds to the Rpn10 promoter and increases its expression in HCC

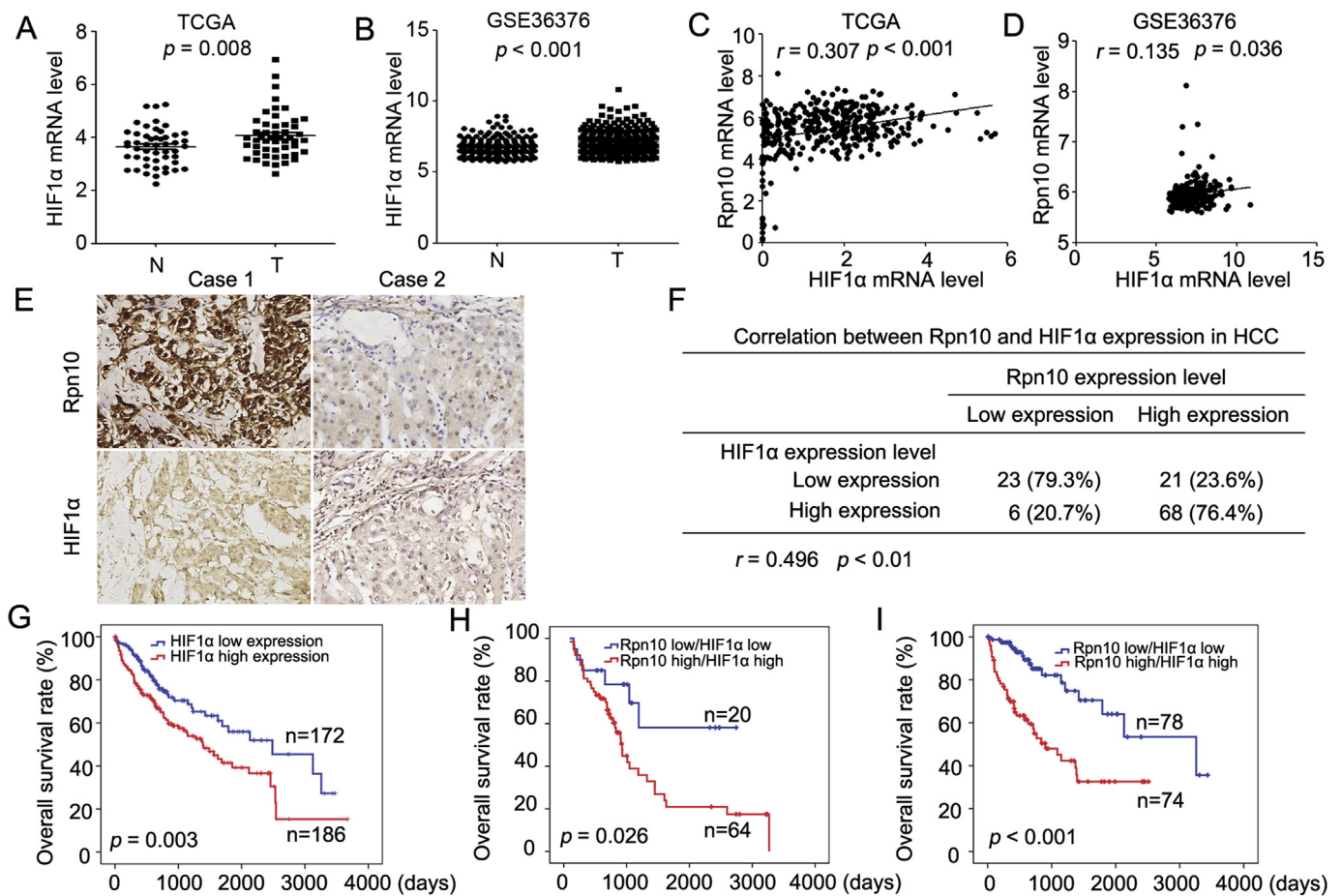


Fig. 7. Rpn10 expression is positively correlated with HIF1α expression in HCC tissues and predicts a poor prognosis. (A) Expression of HIF1α in HCC tissues compared with paired corresponding noncancerous liver tissues was analyzed using data sets from TCGA. (B) Expression of HIF1α in HCC tissues compared with noncancerous liver tissues was analyzed using data sets from GEO. (C) The correlation between Rpn10 expression and HIF1α level was analyzed using data sets from TCGA. $n = 373$; $r = 0.307$; $p < 0.001$. (D) The correlation between Rpn10 expression and HIF1α level was analyzed using data sets from GEO. $n = 240$; $r = 0.135$; $p = 0.036$. (E) IHC analysis of Rpn10 and HIF1α expression in 118 HCC samples. Representative images are shown. (F) The correlation between Rpn10 expression and HIF1α level in 118 HCC tissues was analyzed. (G) Kaplan–Meier curves showing the overall survival of the high and low expression groups based on HIF1α levels according to data sets from TCGA. (H) The combination of Rpn10 and HIF1α increased the probability of a poor prognosis in HCC patients (by the 2-sided log-rank test). (I) The combination of Rpn10 and HIF1α increased the probability of a poor prognosis, according to data sets from TCGA (by the 2-sided log-rank test).

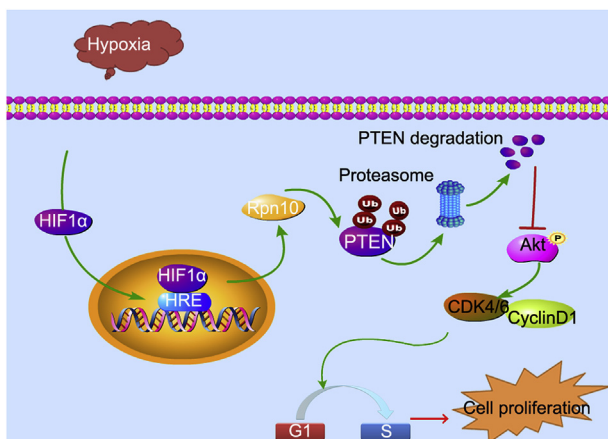


Fig. 8. Model of the mechanisms of action of Rpn10. The transcription factor HIF1α directly binds to the Rpn10 promoter and increases the expression of the gene. Overexpression of Rpn10 directly degrades PTEN expression via the ubiquitin-proteasome pathway and subsequently activates Akt phosphorylation and promotes cell cycle progression in human HCC.

cells (Fig. 8). High Rpn10 and HIF1α levels in HCC patients were associated with poor prognosis. Our findings highlight the molecular mechanism of Rpn10 expression in HCC and provide valuable information for HCC prognosis and treatment.

Conflicts of interest

No potential conflicts of interest were disclosed.

Funding

This work was supported by grants from the National Natural Science Foundation of China (81472570), the Research Project of Shanghai Municipal Health and Family Planning Commission (201540107), and the SKLORG Research Foundation (91-17-29).

Appendix A. Supplementary data

Supplementary data to this article can be found online at <https://doi.org/10.1016/j.canlet.2019.01.020>.

References

- [1] M. Maluccio, A. Covey, Recent progress in understanding, diagnosing, and treating hepatocellular carcinoma, *Ca - Cancer J. Clin.* 62 (2012) 394–399.
- [2] R.L. Siegel, K.D. Miller, A. Jemal, Cancer statistics, 2018, *Ca - Cancer J. Clin.* 68 (2018) 7–30.
- [3] X. Wang, A. Zhang, H. Sun, Power of metabolomics in diagnosis and biomarker discovery of hepatocellular carcinoma, *Hepatology* 57 (2013) 2072–2077.
- [4] M. Shen, S. Schmitt, D. Buac, Q.P. Dou, Targeting the ubiquitin-proteasome system for cancer therapy, *Expert Opin. Ther. Targets* 17 (2013) 1091–1108.
- [5] Y.J. Chen, H. Wu, X.Z. Shen, The ubiquitin-proteasome system and its potential application in hepatocellular carcinoma therapy, *Cancer Lett.* 379 (2016) 245–252.
- [6] G.A. Collins, A.L. Goldberg, The logic of the 26S proteasome, *Cell* 169 (2017) 792–806.
- [7] Y.M. Cheng, P.L. Lin, D.W. Wu, L. Wang, C.C. Huang, H. Lee, PSMD4 is a novel therapeutic target in chemoresistant colorectal cancer activated by cytoplasmic localization of Nrf2, *Oncotarget* 9 (2018) 26342–26352.
- [8] M.S. Fejzo, L. Anderson, H.W. Chen, E. Guandique, O. Kalous, D. Conklin, et al., Proteasome ubiquitin receptor PSMD4 is an amplification target in breast cancer and may predict sensitivity to PARPi, *Genes Chromosomes Cancer* 56 (2017) 589–597.
- [9] J. Godek, I. Sargiannidou, S. Patel, L. Hurd, V.L. Rothman, G.P. Tuszynski, Angiostatin inhibits breast cancer proliferation through activation of epidermal growth factor receptor and nuclear factor kappa (NF- κ B), *Exp. Mol. Pathol.* 90 (2011) 244–251.
- [10] Y. Midorikawa, S. Tsutsumi, H. Taniguchi, M. Ishii, Y. Kobune, T. Kodama, et al., Aburatani. Identification of genes associated with dedifferentiation of hepatocellular carcinoma with expression profiling analysis, *Jpn. J. Canc. Res.* 93 (2002) 636–643.
- [11] H. Tian, C. Ge, H. Li, F. Zhao, H. Hou, T. Chen, et al., Ribonucleotide reductase M2B inhibits cell migration and spreading by early growth response protein 1-mediated phosphatase and tensin homolog/Akt1 pathway in hepatocellular carcinoma, *Hepatology* 59 (2014) 1459–1470.
- [12] H. Hou, C. Ge, H. Sun, H. Li, J. Li, H. Tian, Tunicamycin inhibits cell proliferation and migration in hepatocellular carcinoma through suppression of CD44s and the ERK1/2 pathway, *Cancer Sci.* 109 (2018) 1088–1100.
- [13] H. Tian, C. Ge, F. Zhao, M. Zhu, L. Zhang, Q. Huo, et al., Downregulation of AZGP1 by Ikaros and histone deacetylase promotes tumor progression through the PTEN/Akt and CD44s pathways in hepatocellular carcinoma, *Carcinogenesis* 38 (2017) 207–217.
- [14] X. Wang, L.C. Trotman, T. Koppie, A. Alimonti, Z. Chen, Z. Gao, et al., Erdjument-Bromage, P. Tempst, C. Cordon-Cardo, P.P. Pandolfi, X. Jiang, NEDD4-1 is a proto-oncogenic ubiquitin ligase for PTEN, *Cell* 128 (2007) 129–139.
- [15] K.J. Schmitz, J. Wohlschlaeger, H. Lang, G.C. Sotiropoulos, M. Malago, K. Steveling, et al., Activation of the ERK and AKT signalling pathway predicts poor prognosis in hepatocellular carcinoma and ERK activation in cancer tissue is associated with hepatitis C virus infection, *J. Hepatol.* 48 (2008) 83–90.
- [16] L.M. Chow, S.J. Baker, PTEN function in normal and neoplastic growth, *Cancer Lett.* 241 (2006) 184–196.
- [17] H. Li, C. Ge, F. Zhao, M. Yan, C. Hu, D. Jia, et al., Hypoxia-inducible factor 1 α -activated angiopoietin-like protein 4 contributes to tumor metastasis via vascular cell adhesion molecule-1/integrin β 1 signaling in human hepatocellular carcinoma, *Hepatology* 54 (2011) 910–919.
- [18] P.L. Lin, J.T. Chang, D.W. Wu, C.C. Huang, H. Lee, Cytoplasmic localization of Nrf2 promotes colorectal cancer with more aggressive tumors via upregulation of PSMD4, *Free Radic. Biol. Med.* 95 (2016) 121–132.
- [19] S. Koyasu, M. Kobayashi, Y. Goto, M. Hiraoka, H. Harada, Regulatory mechanisms of hypoxia-inducible factor 1 activity: two decades of knowledge, *Cancer Sci.* 109 (2018) 560–571.
- [20] A.L. Harris, Hypoxia—a key regulatory factor in tumour growth, *Nat. Rev. Canc.* 2 (2002) 38–47.
- [21] H. Zhong, A.M. De Marzo, E. Laughner, M. Lim, D.A. Hilton, D. Zagzag, et al., Overexpression of hypoxia-inducible factor 1 α in common human cancers and their metastases, *Cancer Res.* 59 (1999) 5830–5835.
- [22] J. Zhang, Q. Zhang, Y. Lou, Q. Fu, Q. Chen, T. Wei, et al., Hypoxia-inducible factor-1 α /interleukin-1 β signaling enhances hepatoma epithelial-mesenchymal transition through macrophages in a hypoxic-inflammatory microenvironment, *Hepatology* 67 (2018) 1872–1889.
- [23] M. Wang, X. Zhao, D. Zhu, T. Liu, X. Liang, F. Liu, et al., HIF-1 α promoted vasculogenic mimicry formation in hepatocellular carcinoma through LOXL2 up-regulation in hypoxic tumor microenvironment, *J. Exp. Clin. Oncol.* 36 (2017) 60.
- [24] X. Guo, D. Li, Y. Chen, J. An, K. Wang, Z. Xu, et al., SNP rs2057482 in HIF1A gene predicts clinical outcome of aggressive hepatocellular carcinoma patients after surgery, *Sci. Rep.* 5 (2015) 11846.
- [25] C. Ju, S.P. Colgan, H.K. Eltzschig, Hypoxia-inducible factors as molecular targets for liver diseases, *J. Mol. Med. (Berl.)* 94 (2016) 613–627.
- [26] Z. Wang, C. Fan, H.F. Zhou, J.S. Lu, M.J. Sun, J.W. Song, et al., S5a binds to death receptor-6 to induce THP-1 monocytes to differentiate through the activation of the NF- κ B pathway, *J. Cell Sci.* 127 (2014) 3257–3268.
- [27] A. Sparks, S. Dayal, J. Das, P. Robertson, S. Menendez, M.K. Saville, The degradation of p53 and its major E3 ligase Mdm2 is differentially dependent on the proteasomal ubiquitin receptor S5a, *Oncogene* 33 (2014) 4685–4696.
- [28] J.J. Li, H.K. Yin, D.X. Guan, J.S. Zhao, Y.X. Feng, Y.Z. Deng, et al., Chemerin suppresses hepatocellular carcinoma metastasis through CMKLR1-PTEN-Akt axis, *Br. J. Canc.* 118 (2018) 1337–1348.
- [29] R. Golnik, A. Lehmann, P.M. Kloetzel, F. Ebstein, Major histocompatibility complex (MHC) class I processing of the NY-ESO-1 antigen is regulated by Rpn10 and Rpn13 proteins and immunoproteasomes following non-lysine ubiquitination, *J. Biol. Chem.* 291 (2016) 8805–8815.
- [30] A.S. Lundberg, R.A. Weinberg, Functional inactivation of the retinoblastoma protein requires sequential modification by at least two distinct cyclin-cdk complexes, *Mol. Cell Biol.* 18 (1998) 753–761.
- [31] F. Chang, J.T. Lee, P.M. Navolanic, L.S. Steelman, J.G. Shelton, W.L. Blalock, et al., Involvement of PI3K/Akt pathway in cell cycle progression, apoptosis, and neoplastic transformation: a target for cancer chemotherapy, *Leukemia* 17 (2003) 590–603.
- [32] C. Van Themsche, V. Leblanc, S. Parent, E. Asselin, X-linked inhibitor of apoptosis protein (XIAP) regulates PTEN ubiquitination, content, and compartmentalization, *J. Biol. Chem.* 284 (2009) 20462–20466.
- [33] S.F. Ahmed, S. Deb, I. Paul, A. Chatterjee, T. Mandal, U. Chatterjee, et al., The chaperone-assisted E3 ligase C terminus of Hsc70-interacting protein (CHIP) targets PTEN for proteasomal degradation, *J. Biol. Chem.* 287 (2012) 15996–16006.